Heliyon 9 (2023) e21499

Contents lists available at ScienceDirect

Heliyon

journal homepage: www.cell.com/heliyon

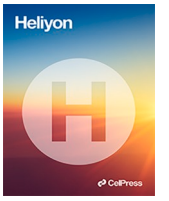

Effect of wall material on lipophilic functional compounds of high oleic palm oil emulsions encapsulated by Refractance Window drying

Alejandra Henao-Ardila [a,b], María Ximena Quintanilla-Carvajal [b], Patricio Román Santagapita [c], Miguel Caldas-Abril [b], Valentina Bonilla-Bravo [b], Fabián Leonardo Moreno [b,*]

[a] *Doctorate in Biosciences, Faculty of Engineering, Universidad de La Sabana, Campus Universitario del Puente del Común, Km7 Autopista Norte de Bogotá, Chía, Cundinamarca, Colombia*
[b] *Grupo de Investigación en Procesos Agroindustriales, Faculty of Engineering, Universidad de La Sabana, Campus Universitario del Puente del Común, Km7 Autopista Norte de Bogotá, Chía, Cundinamarca, Colombia*
[c] *Universidad de Buenos Aires. Facultad de Ciencias Exactas y Naturales. Departamento de Química Orgánica & CIHIDECAR (Centro de Investigaciones en Hidratos de Carbono, CONICET-UBA), Buenos Aires, Argentina*

ARTICLE INFO

Keywords:
Food security
Malnutrition
Carotenoids
Tocopherol
cast tape
Food oil

ABSTRACT

High-oleic palm oil is a food-grade oil with desirable properties, as it is characterised by having an oleic acid concentration above 50 % and a high vitamin E and provitamin A content. This study investigated the effect of different combinations of two wall materials (whey protein (WP) and Capsul®, a commercial octenyl succinic anhydride modified starch (OSA-MS)) on the concentration of provitamin A, vitamin E and oleic acid, and the physical properties of high oleic palm oil emulsions encapsulated by Refractance Window drying technology. Wall material composition significantly affected ($p < 0.05$) all response variables, and R^2 values were above 0.75 for all responses. Phytonutrient preservation showed its highest at an OSA-MS: WP concentration ratio of 1: 3. Optimal results were achieved (minimum moisture content, water activity and hygroscopicity, and maximum encapsulation efficiency and phytonutrient preservation) at an OSA-MS concentration of 8.13 % and WP concentration of 91.87 %. Flakes were obtained as a solid structure that protects oil's phytonutrients with 94 %, 75 % and 87 % of preservation of oleic acid, vitamin E and carotenoids, respectively. It shows that the wall material combination and encapsulation technique are suitable for obtaining lipophilic functional compounds.

1. Introduction

Palm oil is the most produced oil in the world; by 2022, production was more than 73 million tons worldwide [1]. A recent varietal of the palm tree is the hybrid O × G, which produces the oil known as high oleic palm oil (HOPO). The hybrid resulted from the crossing of *Elaeis oleifera* with *Elaeis guineensis*. HOPO has several notable characteristics: (i) a high content of oleic acid, (ii) better content of free fatty acids and (iii) a high content of β-carotene (provitamin A) and vitamin E [2]. Vitamin A and E are metabolites

* Corresponding author.
E-mail address: leonardo.moreno@unisabana.edu.co (F.L. Moreno).

https://doi.org/10.1016/j.heliyon.2023.e21499
Received 1 April 2023; Received in revised form 18 October 2023; Accepted 23 October 2023
Available online 31 October 2023

especially interested in avoiding human malnutrition. However, these phytonutrients are susceptible to thermal degradation, photodegradation and oxidation [3–5]. By subjecting HOPO to refining and transformation processes, a large part of the nutritional and functional content that characterises it can be degraded [6]. Therefore, it can be protected by techniques such as emulsification.

Emulsions encapsulate and transport lipophilic molecules poorly soluble in water [7]. Nevertheless, due to thermodynamical instability, emulsions are difficult to handle in a liquid state [8]. For this reason, a drying stage can be applied to the emulsion. Several technologies, such as spray drying, have been used to dehydrate emulsions [9,10]. Refractance Window (RW) drying is an emerging technology that can dry the emulsion and encapsulate the lipophilic molecules. Refractance Window (RW) drying has emerged as a prominent drying technology that incorporates all modes of heat transfer, ensuring the maintenance of low temperatures while achieving rapid drying. Compared to conventional drying methods like freeze, spray, and convective, RW drying offers several compelling advantages. The most notable benefits include reduced drying time, lower costs, decreased energy consumption, heightened thermal efficiency, low investment costs, and enhanced product quality [11]. These unique advantages position RW drying as an intriguing and promising technology for stabilising O/W emulsions. Its ability to deliver superior product stability and quality results makes it an appealing choice over traditional methods [12]. The efficiency and effectiveness of RW drying hold the potential to provide a stable emulsion product in the form of flakes. The solid-state form of emulsions (flakes) offers significant advantages in handling, providing exciting opportunities for various industries that rely on stable emulsion products.

RW drying has demonstrated remarkable efficiency in preserving phytonutrients, as evidenced by various studies [13–16]. Compared to conventional drying methods like spray drying or convective drying, RW drying stands out [11]. Emulsions in a solid state simplify their handling and ensure the preservation of valuable phytonutrients, making them more suitable for various food applications.

RW drying has been primarily explored in matrices such as fruit pulp, vegetables and sliced fruits [17–20] but has also been studied for the encapsulation of *Lactobacillus fermentum* in a previous work [21]. To date, few authors have reported using RW drying as a technology to stabilise emulsions. In 2010, Cadwallader and collaborators [22] compared the use of RW and spray drying as technologies for encapsulating orange oil, finding that, in general, oil yield was better for RW drying. Previous studies on the effect of process variables on the physical properties and microstructure of HOPO nanoemulsion flakes obtained by RW have been carried out by this research group. The results showed that nanoemulsions obtained at 20,000 psi and dried at 70 °C have flakes with low moisture content and water activity [23].

Final product characteristics, drying efficiency and phytonutrient retention, are affected by wall material selection [24]. A successful drying process must result in a product with a low moisture content and water activity, minimum surface oil and maximum yield of the phytonutrients [24,25]. Wall material for encapsulation should have good solubility, emulsification properties and film-forming ability [26]. Wall materials can act as stabilisers of the lipidic core. Maltodextrin, corn syrup solids and modified starches are common wall materials expected to fulfil that goal [27–30]. Other wall material ingredients, such as proteins, are known for their emulsifying properties; even a minor fraction of protein in specific polysaccharides gives them emulsifying ability, making them appropriate wall materials for encapsulating lipophilic ingredients [31,32]. When heated, proteins allow cross-linking at the oil-water interface [33]. Cross-linking induces the reconfiguration of native macromolecules into three-dimensional structures due to the hydrophobic interactions between the non-polar fragments, the hydrogen bonds and the strong ionic and covalent bonds [9,34]. Whey protein (WP) is a widespread wall material used to encapsulate and protect lipophilic phytonutrients such as carotenoids and tocopherols due to the partial unfolding of the globular protein molecules present in the whey protein isolate, which aggregates to form continuous membranes around oil droplets [34]. Several authors have encapsulated β-carotene [35–39] and tocopherols [40] using whey protein isolate as wall material, reporting good preservation of the active compounds.

On the other hand, polysaccharides such as octenyl succinic anhydride, a modified starch (OSA-MS), are widely used to encapsulate lipophilic phytonutrients [41]. Carneiro et al. (2013), Lin et al. (2018) and Silva et al. (2014) [24,42,43] observed a positive effect on moisture content, protection against gastric conditions and encapsulation efficiency when using OSA-MS as wall material. Combining proteins and polysaccharides is a common practice in producing O/W emulsions. Polysaccharides can be adsorbed onto the surface of protein-coated oil droplets through electrostatic interactions, enhancing emulsions' stability [44]. Investigating the synergistic effect of a protein (WP) and a polysaccharide (OSA-MS) in producing HOPO flakes using RW drying will provide valuable insights into applying these wall materials for encapsulating HOPO. RW drying is a novel technique in emulsion drying, and this study aims to contribute to its development. Understanding the interaction between the chosen protein and polysaccharide in HOPO flake production will pave the way for developing functional flakes with diverse applications in the food industry. These flakes could serve as healthier alternatives to fats, offering consumers more nutritious and appealing choices. Moreover, the potential to incorporate functional ingredients, such as essential fatty acids, vitamins, or antioxidants, further augments the scope for creating innovative food products.

To date, there is a notable gap in research concerning the encapsulation of HOPO through RW drying, employing WP and a commercial OSA-MS (Capsul®) as potential wall materials. As such, the primary objective of this research paper is to investigate and assess the impact of various combinations of WP and Capsul® on the concentration of provitamin A, vitamin E, and oleic acid, as well as the physical properties of HOPO flakes produced through RW drying technology. By delving into this unexplored area of study, we aim to shed light on the potential of RW drying as a novel encapsulation method for HOPO. The evaluation of WP and OSA-MS combinations and their effects on nutrient concentration and physical attributes is vital in unravelling the full potential of this technology.

2. Material and methods

2.1. Raw materials

Emulsions were prepared using crude HOPO which was donated by Hacienda La Cabaña (Fedepalma, Colombia) (oleic acid concentration, total vitamin E and total carotenoid content were 54.6 %, 526.43 ppm and 678.85 ppm, respectively), sweet WP (Moravia Lacto, Czech Republic), Capsul® (Ingredion, USA) and soy lecithin which were purchased at a local market. Ethanol (Scharlau, Spain) and n-hexane (JTBaker, USA) were used to extract superficial and encapsulated oil.

The standards for α, β, δ and γ-tocotrienol, α, β, δ and γ-tocopherol, and α- and β-carotene, which were used for developing the calibration curves, were all purchased from Merck Millipore (USA); the certified standard for oleic acid was purchased from Sigma Aldrich (Supelco® 37 Component FAME Mix).

2.2. Encapsulation

The encapsulation process was carried out in two stages; the first involved preparing an O/W emulsion. The second stage involved the stabilisation of the emulsion through RW drying. Finally, we characterised the solid flakes obtained, as explained in the following sections.

2.2.1. Emulsion preparation

For the preparation of the emulsion (where the goal was to disperse HOPO in an aqueous medium that includes the wall material mixture), the different wall material ratio for each trial (30 % w/w) listed in Table 1 was dissolved in distilled water (53.5 % w/w) at 70 °C using a mixer (Oster, Colombia) for 2 min. HOPO (15 % w/w) was mixed with a constant lecithin concentration (1.5 % w/w) and was added gradually to the dissolved wall material mixture while mixing for 2 min. An LM10 microfluidiser (Microfluidics, England) was then used at a constant pressure of 20,000 psi and 4 cycles to obtain fine emulsion. The ratio of wall material (OSA-MS and/or WP) to HOPO concentration was kept constant at 2:1, as recommended by Ref. [45]. The OSA-MS and WP formulation varied following a binary mixture optimisation design obtained using Design-Expert software version 13.0.2.0 (Stat-Ease Inc., USA) (Table 1), where A was the fraction of OSA-MS and B was the fraction of WP.

Emulsions were prepared following the methodology reported by Ricaurte et al. (2017) [9].

Table 1
Experimental design, physical properties, and lipophilic phytonutrient content of HOPO flakes, and emulsion characterisation.

Wall Material		Emulsion			Flakes						
OSA-MS	WP	ADS (nm)	ζ (mv)	PDI	A	B	C	D	E	F	G
33 %	67 %	488 ± 27.1	−28.5 ± 1.0	0.44 ± 0.11	2.47 % ± 0.2 %	0.27 ± 0.00	57.2 % ± 0.5 %	4.2 % ± 0.1 %	75.9 % ± 0.2 %	82.8 % ± 0.6 %	96.0 % ± 1.6 %
0 %	100 %	265 ± 2.7	−35.6 ± 0.8	0.28 ± 0.03	1.30 % ± 0.2 %	0.17 ± 0.16	88.3 % ± 0.4 %	4.9 % ± 0.1 %	63.9 % ± 1.9 %	69.7 % ± 1.7 %	95.3 % ± 1.4 %
75 %	25 %	352 ± 5.7	−36.4 ± 0.4	0.70 ± 0.06	2.82 % ± 0.1 %	0.33 ± 0.03	64.9 % ± 0.3 %	6.6 % ± 0.1 %	72.6 % ± 0.8 %	72.9 % ± 0.9 %	94.5 % ± 1.1 %
100 %	0 %	124 ± 0.9	−30.7 ± 0.4	0.23 ± 0.02	2.67 % ± 0.2 %	0.2 ± 0.14	72.7 % ± 0.3 %	4.3 % ± 0.1 %	67.2 % ± 0.9 %	78.4 % ± 2.0 %	96.5 % ± 1.7 %
0 %	100 %	250 ± 2.0	−32.0 ± 0.1	0.25 ± 0.00	1.21 % ± 0.1 %	0.17 ± 0.03	87.3 % ± 0.2 %	4.9 % ± 0.0 %	66.8 % ± 0.5 %	84.0 % ± 0.7 %	95.1 % ± 1.5 %
50 %	50 %	327 ± 8.8	−34.8 ± 1.8	0.43 ± 0.03	2.96 % ± 0.2 %	0.28 ± 0.04	28.7 % ± 0.3 %	4.9 % ± 0.1 %	61.6 % ± 1.0 %	79.1 % ± 1.8 %	98.8 % ± 0.9 %
100 %	0 %	124 ± 1.4	−31.1 ± 0.3	0.18 ± 0.02	2.28 % ± 0.0 %	0.21 ± 0.00	74.4 % ± 0.4 %	4.2 % ± 0.0 %	67.8 % ± 2.5 %	69.7 % ± 0.2 %	96.7 % ± 1.3 %
50 %	50 %	434 ± 12.3	−34.2 ± 0.1	0.44 ± 0.02	2.84 % ± 0.2 %	0.28 ± 0.04	25.3 % ± 0.5 %	5.0 % ± 0.1 %	62.4 % ± 0.5 %	81.4 % ± 0.7 %	95.7 % ± 1.7 %
100 %	0 %	124 ± 0.5	−30.8 ± 0.6	0.21 ± 0.00	2.48 % ± 0.4 %	0.2 ± 0.03	62.8 % ± 0.3 %	4.2 % ± 0.1 %	38.9 % ± 3.5 %	50.8 % ± 0.2 %	96.3 % ± 1.2 %
0 %	100 %	205 ± 1.4	−30.3 ± 0.3	0.18 ± 0.01	1.64 % ± 0.0 %	0.17 ± 0.17	87.8 % ± 0.3 %	4.9 % ± 0.1 %	54.7 % ± 3.6 %	66.9 % ± 0.1 %	95.2 % ± 1.5 %
50 %	50 %	370 ± 16.8	−28.3 ± 0.5	0.49 ± 0.04	3.03 % ± 0.2 %	0.28 ± 0.16	25.0 % ± 0.5 %	5.1 % ± 0.0 %	62.7 % ± 1.4 %	77.7 % ± 1.0 %	95.7 % ± 1.9 %
25 %	75 %	514 ± 7.3	−28.3 ± 0.3	0.56 ± 0.13	2.78 % ± 0.3 %	0.28 ± 0.01	65.5 % ± 0.6 %	4.0 % ± 0.0 %	84.6 % ± 2.1 %	83.4 % ± 0.4 %	96.7 % ± 1.2 %
67 %	33 %	230 ± 3.4	−24.0 ± 0.6	0.36 ± 0.02	2.88 % ± 0.4 %	0.31 ± 0.00	42.6 % ± 0.5 %	6.3 % ± 0.1 %	72.6 % ± 2.0 %	73.8 % ± 1.4 %	95.3 % ± 1.7 %

A: Moisture; B: Water activity; C: Encapsulation Efficiency; D: Hygroscopicity; E: Carotenoid retention (%); F: Vitamin E retention (%); G: Oleic acid content (%).

2.2.2. Refractance Window drying

A pilot-scale RW dryer with a capacity of 0.34 kg was utilised to dehydrate HOPO emulsions. The dryer boasts an effective surface drying area of 0.43 m^2 (0.92 m length and 0.36 m width). Its fundamental constituents encompass a tray with a Mylar film 0.5 mm thick (DuPont, USA), a pump 0.5 HP which sends hot water to a chamber below the mylar tray from a hot water tank, a heating unit with a temperature control ($\pm$ 0.01 °C). An acrylic chamber with air extractors covers the tray. Emulsions, with an initial moisture content of 60.0 % $\pm$ 1.0 % w.b, were placed over Mylar film as a thin layer of 1 mm and were left to dry for 1 h in dark conditions. To ensure sample thickness, 14 $\times$ 14 cm frames were placed on the Mylar film and a constant emulsion volume was poured. Drying time and temperature were kept constant at 1 h and 70 °C, respectively, to isolate effects due to drying conditions. Surrounding air presented a relative humidity of 21 % and a temperature of 45 °C. Dry flakes were collected and vacuum-packed in foil bags for no longer than 2 days. Temperature and drying time were established after preliminary tests (data not shown). RW drying was carried out following the methodology Aragón-Rojas et al. (2019) [21] reported.

2.3. Emulsion characterisation

Average droplet size (ADS), zeta potential (ζ) and polydispersity index (PDI) were determined by the dynamic light scattering (DLS) technique to characterise the final emulsion, using a Nano-ZS Zetasizer (Malvern Instruments, England) at a fixed angle of 173° and a 633 nm beam wavelength. Samples were diluted in deionised water at 1: 1000 (v/v) [46].

2.4. Flake quality analysis

2.4.1. Moisture

The moisture content of the obtained flakes was analysed following the thermogravimetric method reported by AOAC [47], where 3 g of dry sample were placed in an oven at 105 °C until no variation in the dry weight was detected ($\pm$0.01g). Moisture was expressed as wet basis percentage (grams of loss water per grams of flakes).

2.4.2. Water activity (a_w)

The a_w was measured using an electronic dew point water activity meter (Decagon Devices, USA) [48].

2.4.3. Hygroscopicity

The hygroscopicity, the ability of a substance to attract and absorb moisture from its surrounding environment, of flake samples was determined according to the method provided by Ribeiro et al. (2019) [49] with some modifications. Briefly, 1 g of the sample was placed in foil dishes and desiccators containing a saturated solution of NaCl (RH: 75.0 %). Dishes were weighed daily until no variation in weight was observed ($\pm$0.01g). Hygroscopicity was expressed as grams of adsorbed moisture per gram of flakes.

2.4.4. Encapsulation efficiency (EEf)

Encapsulation efficiency measured the ratio of non-encapsulated oil vs encapsulated oil, and it was expressed as mg of surface (non-encapsulated) HOPO per mg of encapsulated HOPO. Surface HOPO was extracted by placing on a filter paper (No. 4, Whatman, United Kingdom) 100 mg of flakes and washing them four times with 2.5 mL of n-hexane. The filter was washed with 2 mL of n-hexane to remove residual HOPO. The resulting n-hexane-containing surface HOPO was vacuum-dried in a rotavapor (Heidolph Instruments, Germany) at 150 mbar and 35 °C. Encapsulated HOPO was extracted by adding 4 mL of water to the washed flake and stirring it with a vortex for 2 min. Ethanol (2 mL) and n-hexane (3 mL) were added to the samples and vortexed for 2 min. Samples were then centrifuged at 3500 rpm and 10 °C for 15 min. The organic phase was collected and vacuum-dried in a rotavapor (Heidolph Instruments, Germany) at 150 mbar and 35 °C [50,51].

2.5. Structural characterisation of flakes

2.5.1. SEM micrography

A scanning electron microscope (SEM; Phenom-World, Netherlands) was used to characterise the flakes' surface structure and to see the difference in structure between each wall material. Flakes produced under optimum stabilisation conditions were compared to those from 0: 1 and 1: 0 (OSA-MS/WP) emulsions prepared with no oil. Samples were placed on carbon strips, and images were taken at 1500 $\times$ and 5 kV [52].

2.6. ATR-FTIR spectroscopy

ATR-FTIR spectroscopy was carried out in order to have a better understanding of wall-material interaction. Spectra were acquired in reflectance mode using an Agilent Cary 360 ATR-FTIR analyser (Agilent Scientific Instruments, USA) with an ATR accessory and a ZnSe crystal. They were obtained using 16 scans from 4000 to 650 cm^{-1} with a spectral resolution of 4 cm^{-1}. Backgrounds were collected before every new sample. Spectra were baseline corrected and processed with the free-licence Spectragryph v1.2 software (developed by Dr. Friedrich Menges). Spectra were normalised between 0 and 1 for Fig. presentation. The following controls were taken into account to compare spectra:100%WP with no HOPO, 100%OSA-MS with no HOPO, and 50%WP-50%OSA-MS with no HOPO and HOPO, which were prepared in the same conditions as the other samples.

2.7. Lipophilic phytonutrient quantification

2.7.1. Provitamin A (β-carotene) and vitamin E

In order to evaluate the effect of the encapsulation process on the provitamin A and vitamin E concentration, quantification of provitamin A and vitamin E was carried out through a high-performance liquid chromatography (1260 Infinity, Agilent Technologies, USA) coupled to a fluorescence detector (λ emission: 330 nm, λ excitation: 290 nm) and a diode array detector (λ = 450 nm). Separation was carried out following the method reported by González-Díaz et al. (2021) [53]; the HPLC instrument was equipped with an oven at 30 °C and a Chromolith® RP−18e column in the inverse phase (100–4.6 mm). Mobile phase comprising methanol (Merck Millipore) – Water (Sigma Aldrich) was operated at 1 mL min^{-1}. Results were expressed following Eq. (1) [54].

$$Retention\ (\%) = \frac{ppm\ of\ vitamin\ in\ flake}{ppm\ of\ vitamin\ in\ initial\ HOPO} x100 \quad (1)$$

2.7.2. Oleic acid

Oleic acid was quantified by a gas chromatograph (Agilent Technologies, USA) coupled to a flame ionisation detector. A DB−23 molten silica column (60 m × 0.25 mm (ID) × 0.25 μm (f.t)) coated with a stationary phase of 50 % cyanopropyl–methylpolysiloxane was used, and nitrogen was used as carrier gas. Quantification was done following the methodology reported by González-Díaz et al. (2021) [53], where oleic acid is expressed as the percentage of total fatty acids. The results were presented as residual oleic acid content in the flakes compared to the initial oleic acid content in the HOPO as shown in Eq. (2) [54].

$$Retention\ (\%) = \frac{\%oleic\ acid\ in\ dried\ flake}{\%oleic\ acid\ in\ initial\ HOPO} x100 \quad (2)$$

2.8. Desirability-based optimisation and model validation

A desirability function, a proven approach for determining the most favourable conditions, was employed to find the optimum wall material mix that maximises HOPO phytonutrient retention and encapsulation efficiency and minimises moisture content, a_w and hygroscopicity. The desirability function method involves separating and creating individual functions for each response, which are combined to establish a global function for desired outcomes. The overall effectiveness of the intended responses is ensured by carefully selecting the best values for variables and considering their interactions. The desirability is quantified on a scale from 0 to 1,

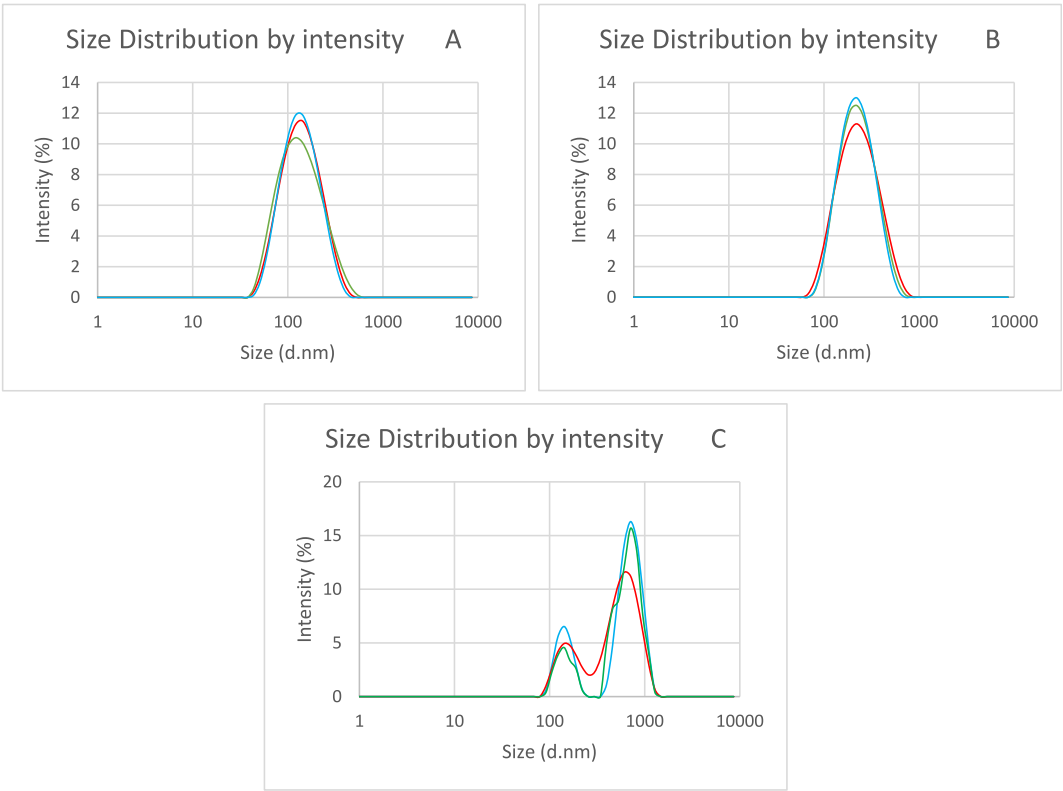

Fig. 1. Average droplet size distribution in emulsions containing **A:** 100 % OSA-MS, **B:** 100 % WP and **C:** 50 % OSA-MS/50 % WP.

Table 2
ANOVA for the variables adjusted to the mixture optimisation design.

Independent factor	Moisture content (%)			a_w			Encapsulation efficiency (%)			Hygroscopicity (%)			Carotenoid retention (%)			Vitamin E retention (%)			Oleic acid retention (%)		
	SS	df	p-value Prob > F	SS	df	p-value Prob > F	SS	df	p-value Prob > F	SS	df	p-value Prob > F	SS	df	p-value Prob > F	SS	df	p-value Prob > F	SS	df	p-value Prob > F
Model	4.38 x 10^{-4}	2	<0.0001	0.039	4	<0.0001	0.63	4	<0.0001	7.49 x 10^{-4}	4	<0.0001	0.072	4	0.0005	0.026	3	0.0023	3.52 x 10^{-4}	3	0.0002
Linear Mixture	1.72 x 10^{-4}	1	<0.0001	3.10 x 10^{-3}	1	<0.0001	0.051	1	0.0015	4.81 x 10^{-9}	1	0.8787	2.85 x 10^{-3}	1	0.1375	1.56 x 10^{-4}	1	0.6689	4.67 x 10^{-5}	1	0.0173
AB	2.62 x 10^{-4}	1	<0.0001	0.018	1	<0.0001	0.58	1	<0.0001	4.06 x 10^{-5}	1	<0.0001	9.61 x 10^{-4}	1	0.3646	0.014	1	0.0022	1.01 x 10^{-4}	1	0.0021
AB(A-B)	–	–	–	8.21 x 10^{-4}	1	0.0001	5.37 x 10^{-5}	1	0.8822	6.26 x 10^{-4}	1	<0.0001	0.0095	1	0.1047	0.012	1	0.0040	2.05 x 10^{-5}	1	0.0002
$AB(A-B)^2$	–	–	–	3.64 x 10^{-3}	1	<0.0001	0.11	1	0.0001	2.94 x 10^{-5}	1	<0.0001	0.0590	1	<0.0001	–	–	–	–	–	–
Lack of Fit	1.89 x 10^{-5}	4	0.3276	6.72 x 10^{-5}	2	0.1257	9.63 x 10^{-3}	2	0.1076	9.17 x 10^{-7}	2	0.0686	0.0003	2	0.8973	8.43 x 10^{-5}	3	0.9945	3.00 x 10^{-5}	3	0.1127
Pure Error	1.97 x 10^{-5}	6	–	6.75 x 10^{-5}	6	–	8.74 x 10^{-3}	6	–	6.36 x 10^{-7}	6	–	0.0081	6	–	7.11 x 10^{-3}	6	–	1.96 x 10^{-5}	6	–
R^2	0.92			1.00			0.97			1.00			0.90			0.78			0.88		
R^2-ajusted	0.90			0.99			0.96			1.00			0.84			0.71			0.84		
Predicted R^2	0.86			0.99			0.89			0.99			0.76			0.53			0.71		

*SS = Sum of Squares, df = degrees of freedom.

where zero represents the least desirable outcome and one signifies the most preferred result. This scale is crucial in determining the comprehensive global function, which can be further enhanced through effective variable selection and optimisation techniques [55]. The desirability function was performed using Design-Expert software (Stat-Ease Inc., USA). All response variables were assigned the same importance value inside the optimisation model. Once the values that optimised the wall material mixture ratio were obtained, the optimal conditions were validated according to sections 2.4 to 2.7.

2.9. Statistical analysis

Following Scheffe's quadratic mixture optimal design model, experiments were carried out using Design-Expert software (Stat-Ease Inc., USA). Two independent variables (OSA-MS (A) and WP (B)) and seven responses (moisture, aw, hygroscopicity, EEf and phytonutrients retention) were selected. Software threw a 13-run design (Table 1.) with 5 lack of fit points and 5 replicate points. The mixture model aims to explore the optimum blends of mixture components, which will provide desirable response characteristics in finished products. Quadratic models were used to express the response variables as a function of the independent factors, where A and B are coded values for OSA-MS and WP, respectively. The significant terms in the model were found through an ANOVA test. The R^2 value evaluated the model's fit. All response tests were performed in triplicate, and the mean and standard deviation values were reported.

3. Results and discussion

3.1. Emulsion characterisation

HOPO emulsions were characterised by measuring ADS, ζ and PDI, shown in Table 1. For ADS, values ranged between 124 and 515 nm, and both wall materials significantly affected ADS. Due to the droplet sizes of the emulsions, which varied between 100 and 500 nm, they can be classified as nanoemulsions [56,57]. Smaller ADS values were obtained when no wall material mixture was used. Higher ADS values were obtained at the lower OSA-MS concentration and decreased as the OSA-MS concentration increased, smaller values being obtained when the OSA-MS concentration reached 100 %. ADS distribution graphs (see Fig. 1) showed a monomodal distribution when no mixture was used (Fig. 1. A, B), showing higher ADS values when using 100 % WP, but when mixtures were made (33 % and higher concentrations of OSA-MS), the graph showed a bimodal distribution (Fig. 1C). These results agree with those obtained for PDI, which increased when wall material mixtures were made. Wu, Lin, Singh, and Ye (2020) [58] reported stable soluble complexes between WP isolate and OSA-MS when the pH value ranged between 4 and 3 (below the isoelectric point of casein). ζ ranged between 24.0 and −36.4 mV, which indicates good electro-kinetic stability. Wall material mixture did not significantly affect ζ values. The results agree with Ricaurte et al. (2016), who also worked with HOPO and WP and obtained ζ values ranging between −29.7 and −47.2 mV.

3.2. Flake quality analysis

Emulsions were prepared following the mixture optimisation design shown in Table 1 and dried at constant operating conditions. The relationship between the different wall material mixtures and their effect on response variables are shown in Table 1. The results showed moisture and a_w values below 5 % and 0.6, respectively, which is desirable for a low rate of deterioration due to microorganisms [59]. EEf varied in a wide range, from 25 % to 88 %, being low when the wall material mixture ratio was 1:1. The results will be further discussed.

All data were analysed by applying multiple regressions using the least squares method. Data were adjusted to different polynomial models (Table 3); adequate fitting of the models was determined by R^2 values above 0.9 for all physical properties, achieving good fit in the models (Table 2), indicating that models adequately describe the process. Table 2 shows the response variables significantly affected by wall material mixtures ($p < 0.05$).

3.2.1. Moisture

Moisture content is an essential attribute in the stability of food powders [60]. Fig. 2A shows that the moisture content of HOPO flakes varied from 1.20 % to 3.03 %, presenting lower values when the WP concentration was highest. It can be seen that the moisture

Table 3
Equations for predicting variables: Moisture content, water activity, Hygroscopicity, Encapsulation efficiency and Carotenoids, vitamin E and oleic acid yield.

Variable	Equation
Moisture content	0.024*[A]+0.014*[B]+0.040*[AB]
Water activity	0.20432*[A]+0.16899*[B]+0.36184*[AB]+0.17944*[AB(A-B)]+1.05394*[AB(A-B)^2]
Hygroscopicity	0.043*[A]+0.049*[B]+0.017*[AB]+0.16*[AB(A-B)]+0.095*[AB(A-B)^2]
Encapsulation efficiency	0.70*[A]+0.88*[B]-2.06*[AB]+0.046*[AB(A-B)]+5.67*[AB(A-B)^2]
Carotenoids yield	0.68*[A]+0.62*[B]-0.084*[AB]-0.37*[AB(A-B)]+4.24*[AB(A-B)^2]
Vitamin E yield	0.74*[A]+0.70*[B]-0.29*[AB]-0.68*[AB(A-B)]
Oleic acid yield	0.95*[A]+0.95*[B]+0.025*[AB]-0.090*[AB(A-B)]

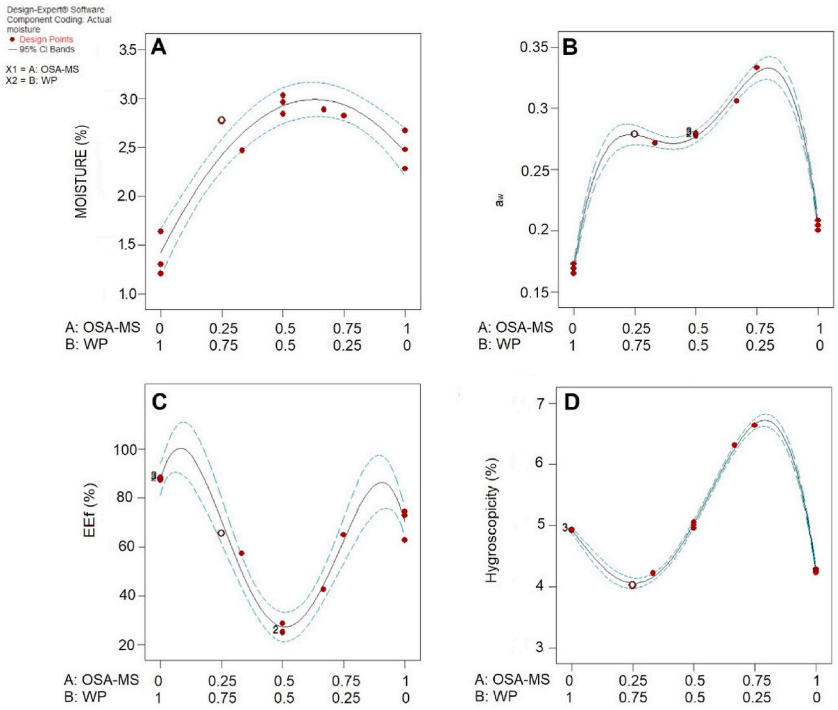

Fig. 2. Effect of wall material concentration on **A:** moisture content, **B:** water activity, **C:** encapsulation efficiency, **D:** hygroscopicity.

content increased as the OSA-MS concentration began to increase; it reached its maximum value when the concentrations of WP and OSA-MS were the same and began to decrease as WP decreased, reaching 2.28 % when only OSA-MS was present. Similar results were obtained by Domian et al. (2018) [61], who encapsulated linseed oil using OSA-MS (Capsul®) as wall material (1.39 % and 1.81 %, w. b.) and Sharif et al. (2017) [62] who encapsulated flax seed using OSA-MS as wall material (1.27–2.25 %). Regarding the mixtures of the two wall materials, the same phenomenon that was previously described for ADS could be observed, which led to obtaining the highest moisture values; however, the moisture content did not exceed 5 %, which is essential for the stability of the flakes since low humidity values imply less microbial growth and a slowdown in the generation of biochemical reactions [59]. Shelke et al. (2023) [63], in their study involving the encapsulation of Jamun juice via spray drying, reported moisture values ranging from 2.57 % to 4.95 %, which is comparatively higher than the moisture content observed in flakes obtained through RW drying. This observation underscores the aptness of RW drying for producing encapsulated lipophilic phytonutrient flakes with notably lower moisture content.

3.2.2. *Water activity (a_w)*

a_w is a crucial response variable when determining the shelf life of dried products; values above 0.6 can lead to microbial deterioration, but values below 0.2 can lead to lipid oxidation [48,64]. For HOPO flakes, a_w ranged between 0.17 and 0.33 (Fig. 2B). a_w presented a similar behaviour to moisture content: lower values were obtained when there was no mixture of wall materials, and the highest value was reached at a concentration ratio of 3:1 (OSA-MS/WP). All a_w values were above 0.6, which means that HOPO flakes are microbiologically stable at every wall material mixture, but a ratio of 0: 1 (WP/OSA-MS and OS-MS/WP) can trigger oxidation processes in the oil since the lowest lipid oxidation rates are found between a_w values between 0.2 and 0.3 [64]. In this sense, OSA-MS showed better results than WP since a_w values of 0.2 were obtained when the OSA-MS was used alone. Mixtures presented a_w values that ranged between 0.28 and 0.33.

3.2.3. *Hygroscopicity*

Dry products with high hygroscopic values can result in moisture accumulation, bacterial growth and the production of odorous substances, which can lead to a loss of nutritional value [65]. Hygroscopicity in HOPO flakes ranged between 4.03 % and 6.63 % (Fig. 2D). According to Schuck, Dolivet, and Jeantet (2012) [66], HOPO flakes can be considered non-hygroscopic since they have hygroscopicity of $<$10 % at 75 % relative humidity. The lowest hygroscopicity value was reached for the mixture of 25 % OSA-MS and increased as WP concentration increased until it reached 4.23 % at 100 % OSA-MS. Hygroscopicity values were lower than those Erdem & Kaya (2021) [59] reported for sunflower oil and WP isolate, which ranged between 13.21 % and 14.20 %. Differences between the two wall materials could be related to the different structures due to the wall materials used [67,68].

3.2.4. *Encapsulation efficiency (EEf)*

EEf was in the range of 25.0 %–88.3 % (Fig. 2C). The lowest EEf value was obtained at the 1: 1 concentration ratio, while the highest

values were achieved for concentration ratios of 1: 0 and 0: 1 (WP: OSA-MS). The EEf when using WP alone was 87.8 %, and when using OSA-MS alone was 70.0 %. High EEf values when using only WP may be due to the whey denaturation process, which creates cross-links with the HOPO, entrapping and protecting the oil. Another possible reason is the system's viscosity; 1: 0 emulsions presented higher viscosity values than 0: 1 emulsions (93.8 and 1.2 mPa s, respectively) (data not shown). Higher viscosity values may reduce particle motion and the probability of oil droplets coalescing [5]. When the emulsion is heated, the particles begin to move faster, which increases the possibility of coalescing, and, as RW drying takes about an hour, if the emulsion has a low viscosity, the oil particles can coalesce and, therefore, decrease the EEf. Results for the 1: 0 concentration ratio are close to those published by Ricaurte et al. (2016) [56] for HOPO encapsulation using WP as a carrier agent (77–99 %). Hategekimana et al. (2015) [69] reported an EEf for Capsul® emulsions obtained by spray drying of 73.15 %, which agrees with our results for the 0: 1 concentration ratio. Similar EEf was reported by Balakrishnan et al. (2021) [70], who encapsulated bixin pigment by spray drying. This result demonstrates that RW drying yields comparable outcomes in oil encapsulation than spray drying. A higher EEf is desirable as it increases the oil loading, prevents core material degradation, and extends shelf life [5].

3.3. Structural characterisation of flakes

3.3.1. SEM micrography

The final product was obtained in the form of flakes. In Fig. 5, it is possible to visualise the OSA-MS (Fig. 5A) and WP (Fig. 5B) without adding HOPO. Fig. 5A shows a smooth and regular structure without forming pores: a sheet with a smooth surface, as described by Soottitantawat et al. (2005) [71]. Small spots of a darker colour can be observed, which may correspond to the soy lecithin added to the mixture. A rougher structure than that observed for OSA-MS is shown in Fig. 5B, but still, no pores are observed: the image shows a continuous film. Darker spots, which may be due to the soy lecithin present in the mixture, can also be observed. When performing the mixture at the optimum concentration ratio (Fig. 5C), the smooth and continuous structure was replaced by a less uniform structure with big cavities, resulting in an amorphous and highly porous structure but still with no small pores. Fig. 5D shows the microstructure of a HOPO flake. In this image, big pores (black spots) may correspond to the air that is incorporated into the emulsion at the moment the emulsion leaves the microfluidiser (the foam that is produced).

Additionally, small pores can also be observed (grey spots). Generally, these small pores should contain the encapsulated oil droplets; the loss of exposed oil in the holes may have occurred due to the vacuum conditions used for SEM observations [71]. Flakes containing all ingredients presented a less homogeneous surface due to the aggregation reactions among the different ingredients [9]. The final flakes are stable. This solid form is an exciting structure to be added to foods as a functional ingredient. This structure can potentially protect the oil's phytonutrients, as discussed in further sections.

3.4. FTIR-ATR spectroscopy

FTIR-ATR spectroscopy was used to investigate the intermolecular interactions between WP and OSA-MS. Fig. 3 shows the FTIR spectra of both wall materials (WP and OSA-MS), their interaction with HOPO, and the interaction between wall materials at 50/50 and the optimum mixture (92/8). For HOPO, the main bands correspond to the asymmetric (2922 cm^{-1}) and symmetric (2854 cm^{-1}) stretching vibration of the methylene group associated with the long-chain fatty acids and to the carbonyl ester group at 1743 cm^{-1}

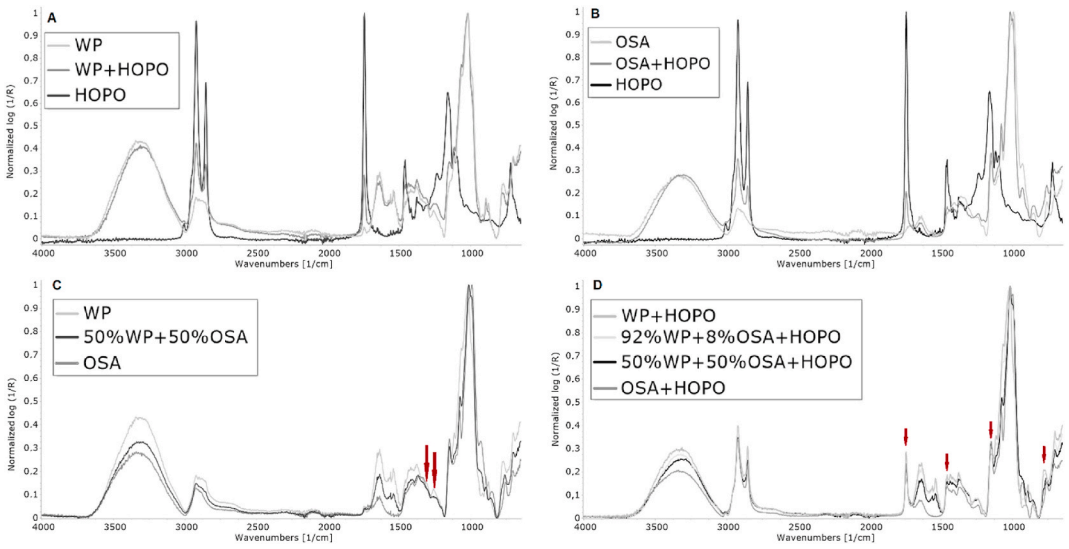

Fig. 3. FTIR-ATR spectra **A:** whey protein, HOPO and whey protein + HOPO, **B:** Capsul, HOPO and Capsul + HOPO, **C:** Whey protein, Capsul and wall material mixture in the ratio 1:1 **D:** Whey protein + HOPO, Capsul + HOPO, wall material mixture in the ratio 1:1 and optimum mixture.

(Fig. 3A and B). The region between 1500 and 600 cm^{-1} represents the C–H and C–O bonds' stretching and bending vibrations. Specifically, the peaks at 1460, 1160 and 720 are related to the C–H scissoring bending of methylene aliphatic groups, C–O stretching of ester groups from the triacylglycerol and the methylene vibration *cis*-disubstituted olefins from unsaturated fatty acids respectively [53,72]. For WP (Fig. 3A), amide I and II bands were found at 1637 and 1541 cm^{-1}, respectively [73]. The region between 1200 and 800 cm^{-1} is a characteristic region for polysaccharide vibrations and contains the main bands, as expected, as the typical stretching of OH is observed between 3000 and 3600 cm^{-1}. In Fig. 3B, the characteristic peaks of the OSA-modified starch occurred at 1718 and 1637 $cm^{-1,}$ which were assigned to the C═O stretching vibration of ester groups and the asymmetric stretching vibration of OSA groups, respectively [10]. HOPO main signals were observed in both WP and OSA mixtures. Moreover, some changes were observed for WP in the presence of HOPO (shifting of signal from 771 cm^{-1} to 779 cm^{-1} Fig. 3A and the OH from 3313 to 3290 cm^{-1}. OSA-HOPO spectra (Fig. 3B) also showed some changes: the main presented a subtle shift from 991 to 999 cm^{-1} and the stretching of the OH from 3340 cm^{-1} to 3297 cm^{-1}.

Some interactions were observed between OSA-MS and WP (Fig. 3C) in the polysaccharide region, indicating an interaction between the lactose from WP and OSA-MS. For the 50%WP-50 % OSA-MS, the bands from WP at 1115 and 1260 cm^{-1} disappeared, indicating possible interaction between both wall materials. No interaction with the protein region was observed. Wu, Lin, Singh, and Ye (2020) [58] found that OSA-MS interacted better with WP when the WP was heated above the denaturation temperature, and pH was above casein's isoelectric point because it increased the hydrophobicity of WP molecules interacting with the OSA-MS, inducing stronger hydrophobic interactions. Since pH was not modified, both wall materials interacted at the hydrophilic region. Interaction between wall materials and HOPO can be observed at 1465 and 1237 cm^{-1} as these HOPO bands disappear when either wall material is used.

In Fig. 3D, the stretching bands from the OH shifted from 3314 cm^{-1} in a 50/50 mixture to 3324 cm^{-1} at the 92/8 (optimum mixture). The bands at 1074 cm^{-1} and 761 cm^{-1} from the 1:1 mixture shifted to 1066 cm^{-1} and 770 cm^{-1} at the optimum mixture. The band at 997 cm^{-1} from the 50/50 mixture (also seen at OSA-HOPO) is no longer visible in the optimum mixture. Changes in 50/50 and 92/8 spectra are due to the higher concentration of WP in the optimum mixture. Several indices were calculated considering significant bands of HOPO and were related to its primary signal at 1743 cm^{-1} (Table 4). The three calculated indices, 1465/1743, 1160/1743, and 721/1743 cm^{-1}, revealed differences among the 50/50 and 92/8 samples, which are unrelated to changes in the composition of the excipients. The $I_{1465/1743}$ shows an increase in the indices in the presence of OSA, WP or both combinations; however, even though the 92/8 sample shows values lower than WP + HOPO, it reveals interactions beyond the physical mixture. The $I_{721/1743}$ and $I_{1160/1743}$ depicted the same behaviour, showing the latter a higher difference between the indices of 50/50 and 92/8 samples. The spectral differences among 50/50 and 92/8 samples could be related to the changes in encapsulation efficiency (Fig. 2) of HOPO.

3.5. Lipophilic phytonutrient quantification

3.5.1. Provitamin A (β-carotene)

During the stabilisation of HOPO emulsions using RW drying, carotenoid retention varied between 54.7 % and 84.6 % (Fig. 4A). Wall material composition had a significative ($p < 0.05$) effect over carotenoid preservation. The carotenoid preservation was better described by a quartic model where the only term that presented a significant effect over carotenoid preservation was $AB(A\text{-}B)^2$; this result suggests that the linear and quadratic effects of factors A and B, as well as interactions with other quartic terms, are not significant compared to the influence of the $AB(A\text{-}B)^2$ interaction on the system's response. The results shown in Fig. 4 show that lower retention values were obtained at the OSA-MS: WP concentration ratios of 1: 0, 0: 1 and 1: 1. When the wall materials were used separately, the preservation of carotenoids was low, but when the concentration ratios of 2: 1, 1: 2, 3: 1 and 1: 3 were used, preservation increased, reaching a maximum value at the mixture ratio of 1: 3 (84.6 %). Results agree with those obtained for EEf, where low concentrations of OSA-MS increased emulsion viscosity, reducing the motility of oil droplets during the drying process and improving oil encapsulation and carotenoid protection. The retention values obtained here are higher than those reported by Ribeiro et al. (2017) [74] who spray-dried carotenoid-rich emulsions, obtaining retention values ranging between 47.89 % and 53.31 %. The highest carotenoid preservation (84.6 %) was achieved using a WP concentration of 75 % and an OSA-MS concentration of 25 %. This WP - OSA-MS ratio allows the production of HOPO flakes with high carotenoid content. This carotenoid retention value surpasses the value reported for spray drying by Ribeiro et al. (2020) [74], where maltodextrin was used as the wall material for carotenoid encapsulation, achieving maximum retention of 53.3 %. It demonstrates that using RW as an emulsion stabilisation technology is an effective technique in carotenoid preservation when employing the WP - OSA-MS combination as wall material.

Table 4
FTIR indexes of 1465, 1160 and 721 cm^{-1} bands related to the main signal at 1743 cm^{-1}.

	$I_{1460/1743}$	$I_{1160/1743}$	$I_{720/1743}$
HOPO	0.454	0.746	0.635
OSA + HOPO	0.595	1.164	0.380
WP + HOPO	0.777	0.678	0.545
50%WP+50%OSA + HOPO	0.817	1.003	0.389
92%WP+8%OSA + HOPO	0.758	0.568	0.356

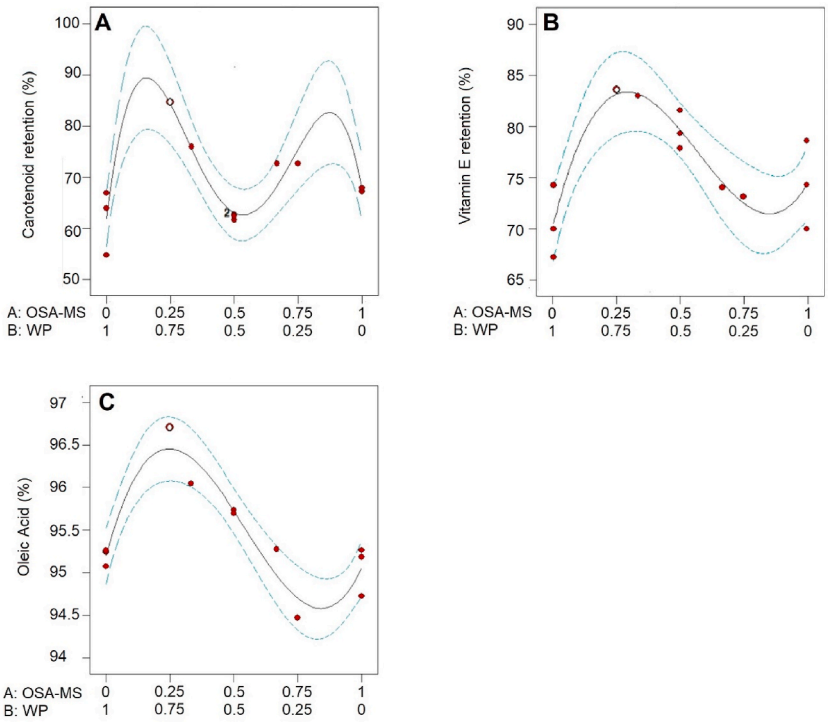

Fig. 4. Effect of wall material concentration on the retention of **A:** carotenoids, **B:** vitamin E, **C:** oleic acid.

3.5.2. Vitamin E

Vitamin E preservation was evaluated, and the results ranged between 83.4 % and 66.9 % for untreated HOPO values, with more remarkable preservation being obtained at an OSA-MS: WP concentration ratio of 1:3 (see Fig. 4B). Wall material composition had a significative ($p < 0.05$) effect over vitamin E preservation. The model that best-described Vitamin E preservation in terms of wall material ratio was a cubic model, where the AB and the AB(A-B) terms presented significant effects over vitamin E preservation, indicating that is not only the linear or quadratic relationship of factors A and B relevant but also the interaction between these factors and how these interactions vary with the difference between A and B. The results agree with those obtained for carotenoid preservation. Lower preservation values were obtained when the wall materials were used alone. Vitamin E preservation reached its maximum value when 25 % OSA-MS was used, the same wall material ratio that preserved carotenoids, but a decreasing trend was evidenced as this percentage increased. OSA-MS was seen to lower emulsion viscosity, resulting in an oily flake. The preservation values obtained are higher than those reported for spray drying by Hategekimana et al. (2015) [69] who obtained α-tocopherol preservation values that ranged between 47 % and 33 % for WP particles and emulsions. It implies that the utilised combination of wall materials effectively safeguards tocopherols and can be employed to develop functional foods with this ingredient.

3.5.3. Oleic acid

Wall material composition had a significative ($p < 0.05$) effect over oleic acid preservation. The model that better describes Oleic acid retention in HOPO flakes is the cubic model, where all terms significatively affected Oleic acid retention. The results shown in Fig. 4C showed retention values ranging between 94.5 % and 98.8 %, indicating good retention at all wall material concentration ratios. However, the higher retention values were obtained at an OSA-MS: WP concentration ratio of 1:3, which agrees with the results obtained for vitamin E and carotenoids. A study carried out in 2020 by Comunian et al. (2020) [75] where the oxidative stability of encapsulated pomegranate oil was evaluated using WP isolate and different combinations with a modified starch (Capsul®) as wall materials. The results showed that the treatment with WP isolate had the highest fatty acid retention, highlighting that the retention of oleic acid was 65.5 %, a lower value than that obtained for stabilised HOPO flakes. The preservation of oleic acid achieved is remarkable. It helps develop functional foods rich in oleic acid in the future.

3.6. Desirability-based optimisation and model validation

With a desirability value of 0.83, the optimal wall material mixture that maximises phytonutrient retention and Eff and minimises moisture, water activity and hygroscopicity were 91.87 % WP and 8.13 % OSA-MS. This wall material mixture produces encapsulated HOPO flakes with the desirable characteristics in Table 5. Desirable characteristics were obtained only at these concentrations: no other mixtures achieved the desirable values. These conditions were replicated to confirm the values predicted by the optimisation

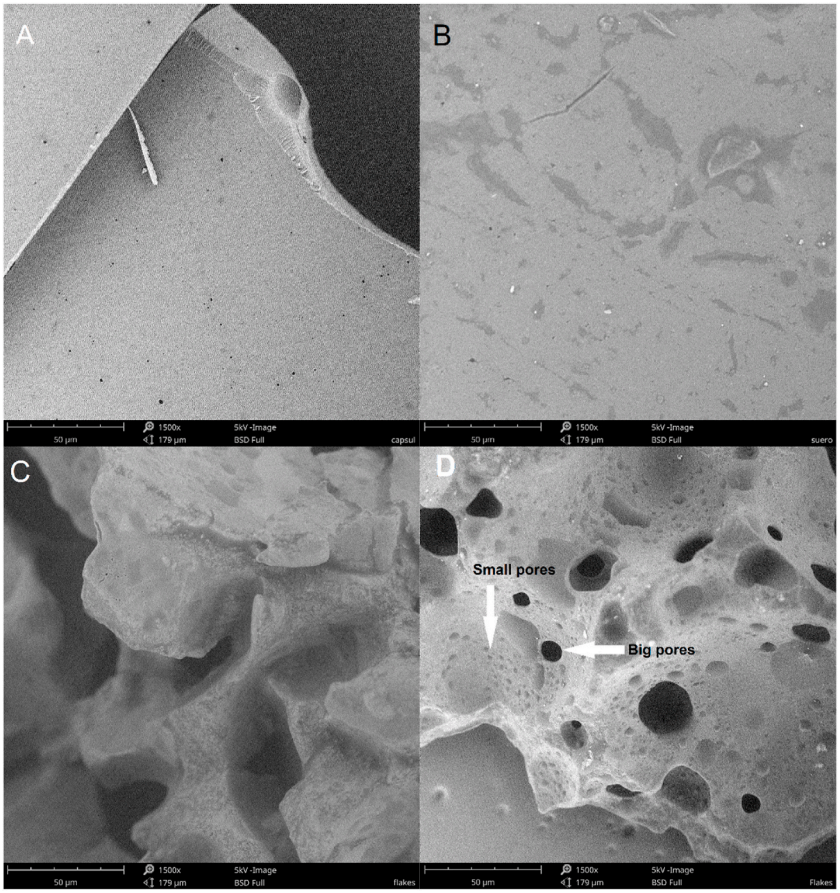

Fig. 5. SEM micrographs for **A:** OSA-MD with no HOPO, **B:** WP with no HOPO, **C:** OSA-MD–WP at optimum concentration ratio with no HOPO, **D:** OSA-MD–WP at optimum concentration ratio with HOPO.

Table 5
Wall material mixture validation at optimal conditions: WP = 91.87 % and OSA-MS = 8.13 %.

	Predicted values	Experimental values	Error
Moisture (%)	1.800	1.871 ± 0.041	−3.94 %
Water Activity	0.2428	0.265 ± 0.013	−9.12 %
Hygroscopicity (%)	4.520	4.403 ± 0,001	2,59 %
Encapsulation efficiency (%)	88.333	85.918 ± 0.001	2.73 %
Carotenoids retention (%)	86.191	87.220 ± 0.049	−1.19 %
Vitamin E retention (%)	76.957	75.115 ± 0.006	2.39 %
Oleic Acid (%)	95.925	93.888 ± 0.005	2.12 %

model. The predicted and experimental values for the optimum conditions are shown in Table 5. The results presented low error values, and the ANOVA test indicated no significant difference among results, which shows the suitability of the D-optimal design model for the optimisation of wall material mixture concentrations to produce HOPO flakes. Even though it was possible to obtain HOPO flakes with high phytonutrient content, it is essential to highlight that these conditions might not be replicated in other lipid matrices and/or with a different wall material combination. Therefore, it is important to study other food matrices. Additionally, RW drying offers advantages over other drying techniques since RW drying was developed to address and mitigate the existing drawbacks associated with drying systems, encompassing aspects such as installation costs, drying expenses, drying duration, and safeguarding product integrity, among others. Some disadvantages could include scalability and production capacity [76].

A stable product in the form of flakes was obtained at the optimal conditions. A high preservation of functional compounds is achieved under this condition. This result shows the convenience of the reactance window drying to stabilised oil emulsions. This drying method is energy efficient, and further economic analysis is suggested to evaluate the feasibility [11,77].

4. Conclusions

It was possible to encapsulate HOPO emulsions using WP and OSA-MS as wall materials using RW drying. Wall material concentration significantly affects all physical properties. When WP or OSA-MS was used alone, lower moisture content values, aw, and hygroscopicity were achieved. Increasing OSA-MS concentration in the wall material mixture increased moisture content and a_w and decreased EEf. It could happen due to the lower viscosity of the emulsion. Interactions between both wall materials were observed at the polysaccharide region, reducing the interaction at the hydrophobic region. Reducing pH might improve these interactions; therefore, studying the interaction between both wall materials and the HOPO in depth is crucial. On the other hand, low OSA-MS concentrations increased the retention of carotenoids, vitamin E and oleic acid, showing higher retention values than those reported by other authors. Although the emulsions dehydrated using RW drying do not show phase separation, it is essential to study their behaviour over time to determine the stability of the flakes.

The optimal combination of wall materials and RW drying technology enables the preservation of carotenoids at 86.2 %, Vitamin E at 77.0 %, and oleic acid at 96.0 %. It demonstrates that the technique is suitable for producing functional HOPO flakes for functional lipid-based ingredients. This research opens doors to producing advanced food formulations that align with the growing demand for healthier and functional food options.

Data availability statement

Data will be made available on request.

CRediT authorship contribution statement

Alejandra Henao-Ardila: Conceptualization, Data curation, Formal analysis, Investigation, Writing – original draft. **María Ximena Quintanilla-Carvajal:** Conceptualization, Formal analysis, Supervision, Validation, Writing – review & editing. **Patricio Román Santagapita:** Conceptualization, Formal analysis, Investigation, Writing – review & editing. **Miguel Caldas-Abril:** Formal analysis, Investigation. **Valentina Bonilla-Bravo:** Formal analysis, Investigation. **Fabián Leonardo Moreno:** Conceptualization, Formal analysis, Funding acquisition, Methodology, Project administration, Resources, Supervision, Writing – review & editing.

Declaration of competing interest

The authors declare that they have no known competing financial interests or personal relationships that could have appeared to influence the work reported in this paper.

Acknowledgements

This research was funded by the Universidad de La Sabana under project ING-206-2018. The first author thanks Universidad de La Sabana for the grant awarded for her doctoral studies.

References

[1] U.S. Department, Of Agriculture, Palm Oil Explorer, 2023. https://ipad.fas.usda.gov/cropexplorer/cropview/commodityView.aspx?cropid=4243000. (Accessed 4 August 2023).
[2] C. Montoya, B. Cochard, A. Flori, D. Cros, R. Lopes, T. Cuellar, S. Espeout, I. Syaputra, P. Villeneuve, M. Pina, E. Ritter, Genetic architecture of palm oil fatty acid composition in cultivated oil palm (Elaeis guineensis Jacq.) compared to its wild relative E. oleifera (HBK) Cortés, PLoS One 9 (2014), e95412.
[3] V. Raikos, Encapsulation of vitamin E in edible orange oil-in-water emulsion beverages: influence of heating temperature on physicochemical stability during chilled storage, Food Hydrocoll 72 (2017) 155–162, https://doi.org/10.1016/j.foodhyd.2017.05.027.
[4] J. Han, Z. Zhang, W. Shang, J. Yan, D. Julian McClements, H. Xiao, H. Wu, B. Zhu, Modulation of physicochemical stability and bioaccessibility of β-carotene using alginate beads and emulsion stabilized by scallop (Patinopecten yessoensis) gonad protein isolates, Food Res. Int. 129 (2020), https://doi.org/10.1016/j.foodres.2019.108875.
[5] S. Raeisi, S.M. Ojagh, S.Y. Quek, P. Pourashouri, F. Salaün, Nano-encapsulation of fish oil and garlic essential oil by a novel composition of wall material: Persian gum-chitosan, LWT - Food Sci. Technol. (Lebensmittel-Wissenschaft -Technol.) 116 (2019), https://doi.org/10.1016/j.lwt.2019.108494.
[6] M. Srimiati, C.M. Kusharto, I. Tanziha, S.H. Suseno, Effect of different bleaching temperatures on the quality of refined catfish (Clarias gariepinus) oil, Procedia Food Sci 3 (2015) 223–230, https://doi.org/10.1016/J.PROFOO.2015.01.025.
[7] M. Saifullah, M.R.I. Shishir, R. Ferdowsi, M.R. Tanver Rahman, Q. Van Vuong, Micro and nano encapsulation, retention and controlled release of flavor and aroma compounds: a critical review, Trends Food Sci. Technol. 86 (2019) 230–251, https://doi.org/10.1016/j.tifs.2019.02.030.
[8] S. Roohinejad, I. Oey, J. Wen, S.J. Lee, D.W. Everett, D.J. Burritt, Formulation of oil-in-water B-carotene microemulsions: effect of oil type and fatty acid chain length, Food Chem. (2015) 270–278, https://doi.org/10.1016/j.foodchem.2014.11.056.
[9] L. Ricaurte, R.E. Prieto Correa, M. de Jesus Perea-Flores, M.X. Quintanilla-Carvajal, Influence of milk whey on high-oleic palm oil nanoemulsions: powder production, physical and release properties, Food Biophys. 12 (2017) 439–450, https://doi.org/10.1007/s11483-017-9500-9.
[10] S. Fang, X. Zhao, Y. Liu, X. Liang, Y. Yang, Fabricating multilayer emulsions by using OSA starch and chitosan suitable for spray drying: application in the encapsulation of β-carotene, Food Hydrocoll 93 (2019) 102–110, https://doi.org/10.1016/j.foodhyd.2019.02.024.
[11] N. Kumar Mahanti, S.K. Chakraborty, A. Sudhakar, D. Kumar Verma, S. Shankar, M. Thakur, S. Singh, S. Tripathy, A. Kumar Gupta, P. Srivastav, N.K. Mahanti, D.K. Verma, S.K. Chakraborty, A. Sudhakar, Refractance Window TM-Drying vs. other drying methods and effect of different process parameters on quality of foods: a comprehensive review of trends and technological developments://creativecommons.org/licenses/by/4.0/), Future Foods 3 (2021), 100024, https://doi.org/10.1016/j.fufo.2021.100024.
[12] E. Rurush, M. Alvarado, P. Palacios, Y. Flores, M.L. Rojas, A.C. Miano, Drying Kinetics of Blueberry Pulp and Mass Transfer Parameters: Effect of Hot Air and Refractance Window Drying at Different Temperatures, 2021, https://doi.org/10.1016/j.jfoodeng.2021.110929.

[13] B. Nayak, J.J. Berrios, J.R. Powers, J. Tang, Y. Ji, Colored potatoes (Solanum tuberosum L.) dried for antioxidant-rich value- added foods, J. Food Process. Preserv. 35 (2011) 571–580, https://doi.org/10.1111/j.1745-4549.2010.00502.x.

[14] V. Baeghbali, M. Niakousari, Evaluation of a batch refractance window dryer in drying of some heat sensitive food stuff, Iranian Journal of Food Science and Technology 13 (2015) 185–192.

[15] F. Samia El-Safy, Drying characteristics of loquat slices using different dehydration methods by comparative evaluation, World J. Dairy Food Sci. 9 (2014) 272–284, https://doi.org/10.5829/idosi.wjdfs.2014.9.2.9122.

[16] C.I. Nindo, T. Sun, S.W. Wang, J. Tang, J.R. Powers, Evaluation of drying technologies for retention of physical quality and antioxidants in asparagus (Asparagus officinalis, L.), LWT - Food Sci. Technol. (Lebensmittel-Wissenschaft -Technol.) 36 (2003) 507–516, https://doi.org/10.1016/S0023-6438(03)00046-X.

[17] L. Puente, A. Vega-Gálvez, K.S. Ah-Hen, A. Rodríguez, A. Pasten, J. Poblete, C. Pardo-Orellana, M. Muñoz, Refractance Window drying of goldenberry (Physalis peruviana L.) pulp: a comparison of quality characteristics with respect to other drying techniques, LWT - Food Sci. Technol. (Lebensmittel-Wissenschaft -Technol.) (2020) 131, https://doi.org/10.1016/j.lwt.2020.109772.

[18] D. Rajoriya, S.R. Shewale, H.U. Hebbar, Refractance window drying of apple slices: mass transfer phenomena and quality parameters, Food Bioproc Tech 12 (2019) 1646–1658, https://doi.org/10.1007/s11947-019-02334-7.

[19] D. Rajoriya, S.R. Shewale, M.L. Bhavya, H.U. Hebbar, Far infrared assisted refractance window drying of apple slices: comparative study on flavour, nutrient retention and drying characteristics, Innovative Food Sci. Emerging Technol. 66 (2020) 1466–8564, https://doi.org/10.1016/j.ifset.2020.102530.

[20] L.M.M. Raghavi, J.A.A. Moses, C. Anandharamakrishnan, Refractance window drying of foods: a review, J. Food Eng. 222 (2018) 267–275, https://doi.org/10.1016/j.jfoodeng.2017.11.032.

[21] S. Aragón-Rojas, M.X. Quintanilla-Carvajal, H. Hernández-Sánchez, A.J. Hernández-Álvarez, F.L. Moreno, Encapsulation of Lactobacillus fermentum K73 by refractance window drying, Sci. Rep. 9 (2019) 1–15, https://doi.org/10.1038/s41598-019-42016-0.

[22] K.R. Cadwallader, J.J. Moore, Z. Zhang, S.J. Schmidt, Comparison of spray drying and refractance window drying tchnologies for the encapsulation of Orange oil, in: C.T. Ho, C.J. Mussinan, F. Shahidi, E. Tratas Contis (Eds.), Recent Advances in Food and Flavour Chemestry, RSCPublishing, 2010, pp. 256–264.

[23] M. Hernández-Carrión, M. Moyano-Molano, L. Ricaurte, A. Clavijo-Romero, M.X. Quintanilla-Carvajal, The effect of process variables on the physical properties and microstructure of HOPO nanoemulsion flakes obtained by refractance window, Sci. Rep. 11 (2021) 1–14.

[24] H.C.F. Carneiro, R.V. Tonon, C.R.F. Grosso, M.D. Hubinger, Encapsulation efficiency and oxidative stability of flaxseed oil microencapsulated by spray drying using different combinations of wall materials, J. Food Eng. 115 (2013) 443–451, https://doi.org/10.1016/j.jfoodeng.2012.03.033.

[25] S.M. Jafari, E. Assadpoor, Y. He, B. Bhandari, Encapsulation efficiency of food flavours and oils during spray drying, Dry. Technol. 26 (2008) 816–835, https://doi.org/10.1080/07373930802135972.

[26] A.S. Prata, L. Garcia, R.V. Tonon, M.D. Hubinger, Wall material selection for encapsulation by spray drying, Journal of Colloid Science and Biotechnology 2 (2013) 86–92, https://doi.org/10.1166/jcsb.2013.1039.

[27] T. Matsuura, A. Ogawa, M. Tomabechi, R. Matsushita, S. Gohtani, T.L. Neoh, H. Yoshii, Effect of dextrose equivalent of maltodextrin on the stability of emulsified coconut-oil in spray-dried powder, J. Food Eng. 163 (2015) 54–59, https://doi.org/10.1016/j.jfoodeng.2015.04.018.

[28] Z. Xiao, Y. Kang, W. Hou, Y. Niu, X. Kou, Microcapsules based on octenyl succinic anhydride (OSA)-modified starch and maltodextrins changing the composition and release property of rose essential oil, Int. J. Biol. Macromol. 137 (2019) 132–138, https://doi.org/10.1016/j.ijbiomac.2019.06.178.

[29] J.S.F. de Araújo, E.L. de Souza, J.R. Oliveira, A.C.A. Gomes, L.R.V. Kotzebue, D.L. da Silva Agostini, D.L.V. de Oliveira, S.E. Mazzetto, A.L. da Silva, M. T. Cavalcanti, Microencapsulation of sweet orange essential oil (Citrus aurantium var. dulcis) by liophylization using maltodextrin and maltodextrin/gelatin mixtures: preparation, characterization, antimicrobial and antioxidant activities, Int. J. Biol. Macromol. 143 (2020) 991–999, https://doi.org/10.1016/j.ijbiomac.2019.09.160.

[30] E. Assadpour, Y. Maghsoudlou, S.-M. Jafari, M. Ghorbani, M. Aalami, Optimization of folic acid nano-emulsification and encapsulation by maltodextrin-whey protein double emulsions, Int. J. Biol. Macromol. 86 (2016) 197–207, https://doi.org/10.1016/j.ijbiomac.2016.01.064.

[31] Z.E. Sikorski, Proteins, in: Z.E. Sikorski (Ed.), Chemical and Functional Properties of Food Components, CRC Press, Boca Raton, 2006, pp. 134–173, https://doi.org/10.1017/CBO9781107415324.004.

[32] C. Anandharamakrishnan, S. Padma-Ishwarya, Selection of wall material for encapsulation by spray drying, in: Spray Drying Techniques for Food Ingredient Encapsulation, John Wiley and Sons, 2015, pp. 77–100, https://doi.org/10.1002/9781118863985.ch4.

[33] A. Sarkar, J. Arfsten, P.-A.A. Golay, S. Acquistapace, E. Heinrich, Microstructure and long-term stability of spray dried emulsions with ultra-high oil content, Food Hydrocoll 52 (2016) 857–867, https://doi.org/10.1016/j.foodhyd.2015.09.003.

[34] L. Wang, Y. Gao, J. Li, M. Subirade, Y. Song, L. Liang, Effect of resveratrol or ascorbic acid on the stability of α-tocopherol in O/W emulsions stabilized by whey protein isolate: simultaneous encapsulation of the vitamin and the protective antioxidant, Food Chem. 196 (2016) 466–474, https://doi.org/10.1016/j.foodchem.2015.09.071.

[35] S. Mun, S. Park, Y.R. Kim, D.J. McClements, Influence of methylcellulose on attributes of β-carotene fortified starch-based filled hydrogels: optical, rheological, structural, digestibility, and bioaccessibility properties, Food Res. Int. 87 (2016) 18–24, https://doi.org/10.1016/j.foodres.2016.06.008.

[36] L.G. Gómez-Mascaraque, R. Perez-Masiá, R. González-Barrio, M.J. Periago, A. López-Rubio, Potential of microencapsulation through emulsion-electrospraying to improve the bioaccesibility of β-carotene, Food Hydrocoll 73 (2017) 1–12, https://doi.org/10.1016/j.foodhyd.2017.06.019.

[37] B. Mehrad, R. Ravanfar, J. Licker, J.M. Regenstein, A. Abbaspourrad, Enhancing the physicochemical stability of β-carotene solid lipid nanoparticle (SLNP) using whey protein isolate, Food Res. Int. 105 (2018) 962–969, https://doi.org/10.1016/j.foodres.2017.12.036.

[38] M. Iddir, C. Degerli, G. Dingeo, C. Desmarchelier, T. Schleeh, P. Borel, Y. Larondelle, T. Bohn, Whey protein isolate modulates beta-carotene bioaccessibility depending on gastro-intestinal digestion conditions, Food Chem. (2019) 157–166, https://doi.org/10.1016/j.foodchem.2019.04.003.

[39] D. Xu, X. Wang, J. Jiang, F. Yuan, Y. Gao, Impact of whey protein - beet pectin conjugation on the physicochemical stability of b-carotene emulsions, Food Hydrocoll (2012) 258–266, https://doi.org/10.1016/j.foodhyd.2012.01.002.

[40] Z. Fang, X. Xu, H. Cheng, J. Li, C. Guang, L. Liang, Comparison of whey protein particles and emulsions for the encapsulation and protection of α-tocopherol, J. Food Eng. 247 (2019) 56–63, https://doi.org/10.1016/j.jfoodeng.2018.11.028.

[41] P.A. Williams, M. Kamran, M. Aslam, H. Majeed, W. Safdar, M. Shamoon, M. Shoaib, J. Haider, F. Zhong, Influence of OSA-starch on the physico chemical characteristics of fl ax seed oil-eugenol nanoemulsions, Food Hydrocoll 66 (2017) 365–377.

[42] V.M. Silva, G.S. Vieira, M.D. Hubinger, Influence of different combinations of wall materials and homogenisation pressure on the microencapsulation of green coffee oil by spray drying, Food Res. Int. 61 (2014) 132–143, https://doi.org/10.1016/j.foodres.2014.01.052.

[43] Q. Lin, R. Liang, F. Zhong, A. Ye, H. Singh, Effect of degree of octenyl succinic anhydride (OSA) substitution on the digestion of emulsions and the bioaccessibility of β-carotene in OSA-modified-starch-stabilized-emulsions, Food Hydrocoll 84 (2018) 303–312, https://doi.org/10.1016/j.foodhyd.2018.05.056.

[44] E. Dickinson, Interfacial structure and stability of food emulsions as affected byprotein–polysaccharide interactions, Soft Matter 4 (2008) 932–942, https://doi.org/10.1039/b800106e.

[45] M. Hernandez-Carrión, M. Moyano, M.X. Quintanilla-Carvajal, Design of high-oleic palm oil nanoemulsions suitable for drying in refractance window™, J. Food Process. Preserv. 45 (2021), https://doi.org/10.1111/jfpp.15076, 0–2.

[46] J.D. Beltrán, C.E. Sandoval-Cuellar, K. Bauer, M.X. Quintanilla-Carvajal, In-vitro digestion of high-oleic palm oil nanoliposomes prepared with unpurified soy lecithin: physical stability and nano-liposome digestibility, Colloids Surf. A Physicochem. Eng. Asp. 578 (2019), https://doi.org/10.1016/j.colsurfa.2019.123603.

[47] Aoac, Official Methods of Analysis of AOAC International, twentieth ed., AOAC international, Maryland, USA., 2016.

[48] A. Henao-Ardila, M.X. Quintanilla-Carvajal, F.L. Moreno, Combination of freeze concentration and spray drying for the production of feijoa (Acca sellowiana b.) pulp powder, Powder Technol. 344 (2019) 190–198, https://doi.org/10.1016/j.powtec.2018.12.015.

[49] L. Carneiro Ribeiro, J.M. Correia da Costa, M. Rodrigues Amorim Afoso, Hygroscopic behavior of acerola powder obtained by spray-drying, Acta Scientiarium Technology 41 (2019) 3–8.

[50] M.X. Quintanilla Carvajal, L.S. Meraz Torres, L. Alamilla Beltrán, J.J. Chanona Pérez, E. Terres Rojas, H. Hernández Sánchez, A.R. Jiménez Aparicio, G. F. Gutiérrez López, Caracterización morfométrica de microcápsulas secadas por aspersión antes y después de la extracción de α-tocoferol, Rev. Mex. Ing. Quim. 10 (2011) 301–312. http://www.scielo.org.mx/scielo.php?script=sci_arttext&pid=S1665-27382011000200014&lng=es&nrm=iso&tlng=en. (Accessed 2 September 2015).
[51] E.H.J. Kim, X.D. Chen, D. Pearce, Surface composition of industrial spray-dried milk powders. 2. Effects of spray drying conditions on the surface composition, J. Food Eng. 94 (2009) 169–181, https://doi.org/10.1016/j.jfoodeng.2008.10.020.
[52] F.L. Moreno, A. Henao-ardila, L. Ricaurte, M.X. Quintanilla-Carvajal, Effect of two atomization devices on the particle size of feijoa pulp powder obtained by spray drying, in: Proceedings of Eurodrying'2019, Italy, Torino, 2019, pp. 10–15.
[53] A. Gonzalez-Diaz, A. Pataquiva-Mateus, J.A. García-Núñez, Characterization and response surface optimization driven ultrasonic nanoemulsification of oil with high phytonutrient concentration recovered from palm oil biodiesel distillation, Colloids Surf. A Physicochem. Eng. Asp. 612 (2021), https://doi.org/10.1016/j.colsurfa.2020.125961.
[54] F. Yu, Z. Li, T. Zhang, Y. Wei, Y. Xue, C. Xue, Influence of encapsulation techniques on the structure, physical properties, and thermal stability of fish oil microcapsules by spray drying, J. Food Process. Eng. 40 (2017), https://doi.org/10.1111/jfpe.12576.
[55] P. Sharma, M. Sivaramakrishnaiah, B. Deepanraj, R. Saravanan, M.V. Reddy, A novel optimization approach for biohydrogen production using algal biomass, Int. J. Hydrogen Energy (2022), https://doi.org/10.1016/J.IJHYDENE.2022.09.274.
[56] L. Ricaurte, M.D.J. Perea-Flores, A. Martinez, M.X. Quintanilla-Carvajal, Production of high-oleic palm oil nanoemulsions by high-shear homogenization (microfluidization), Innovative Food Sci. Emerging Technol. 35 (2016) 75–85, https://doi.org/10.1016/j.ifset.2016.04.004.
[57] X. Xin, H. Zhang, G. Xu, Y. Tan, J. Zhang, X. Lv, Influence of CTAB and SDS on the properties of oil-in-water nano-emulsion with paraffin and span 20/Tween 20, Colloids Surf. A Physicochem. Eng. Asp. 418 (2013) 60–67, https://doi.org/10.1016/j.colsurfa.2012.10.065.
[58] D. Wu, Q. Lin, H. Singh, A. Ye, Complexation between whey protein and octenyl succinic anhydride (OSA)-modified starch: formation and characteristics of soluble complexes, Food Res. Int. 136 (2020), https://doi.org/10.1016/j.foodres.2020.109350.
[59] B.G. Erdem, S. Kaya, Production and application of freeze dried biocomposite coating powders from sunflower oil and soy protein or whey protein isolates, Food Chem. 339 (2021), https://doi.org/10.1016/j.foodchem.2020.127976.
[60] R.G.K. Lekshmi, M. Rahima, N.S. Chatterjee, C.S. Tejpal, K.K. Anas, K.V. Vishnu, K. Sarika, K.K. Asha, R. Anandan, M. Suseela, Chitosan – whey protein as efficient delivery system for squalene: characterization and functional food application, Int. J. Biol. Macromol. 135 (2019) 855–863, https://doi.org/10.1016/j.ijbiomac.2019.05.153.
[61] E. Domian, J. Cenkier, A. Górska, A. Brynda-Kopytowska, Effect of oil content and drying method on bulk properties and stability of powdered emulsions with OSA starch and linseed oil, LWT - Food Sci. Technol. (Lebensmittel-Wissenschaft -Technol.) 88 (2018) 95–102, https://doi.org/10.1016/j.lwt.2017.09.043.
[62] H.R. Sharif, H.D. Goff, H. Majeed, F. Liu, J. Nsor-Atindana, J. Haider, R. Liang, F. Zhong, Physicochemical stability of β-carotene and α-tocopherol enriched nanoemulsions: influence of carrier oil, emulsifier and antioxidant, Colloids Surf. A Physicochem. Eng. Asp. 529 (2017) 550–559, https://doi.org/10.1016/j.colsurfa.2017.05.076.
[63] G. Shelke, V. Kad, R. Pandiselvam, G. Yenge, S. Kakade, S. Desai, R. Kukde, P. Singh, Physical and functional stability of spray-dried jamun (Syzygium cumini L.) juice powder produced with different carrier agents, J. Texture Stud. (2023), https://doi.org/10.1111/JTXS.12749.
[64] T.P. Vu, L. He, D.J. McClements, E.A. Decker, Effects of water activity, sugars, and proteins on lipid oxidative stability of low moisture model crackers, Food Res. Int. (2020), https://doi.org/10.1016/j.foodres.2019.108844.
[65] X. Li, R. Yang, H. Ju, K. Wang, S. Lin, Identification of dominant spoilage bacteria in sea cucumber protein peptide powders (SCPPs) and methods for controlling the growth of dominant spoilage bacteria by inhibiting hygroscopicity, Sci. Technol. 136 (2021), https://doi.org/10.1016/j.lwt.2020.110355.
[66] P. Schuck, A. Dolivet, R. Jeantet, Analytical Methods for Food and Dairy Powders, Wley-Blackwell, 2012, https://doi.org/10.1002/9781118307397.
[67] A. Bassijeh, S. Ansari, S.M.H. Hosseini, Astaxanthin encapsulation in multilayer emulsions stabilized by complex coacervates of whey protein isolate and Persian gum and its use as a natural colorant in a model beverage, Food Res. Int. 137 (2020) 963–9969, https://doi.org/10.1016/j.foodres.2020.109689.
[68] F.C. Da Silva, C.R. Da Fonseca, S.M. De Alencar, M. Thomazini, J.C.D.C. Balieiro, P. Pittia, C.S. Favaro-Trindade, Assessment of production efficiency, physicochemical properties and storage stability of spray-dried propolis, a natural food additive, using gum Arabic and OSA starch-based carrier systems, Food Bioprod. Process. 91 (2013) 28–36, https://doi.org/10.1016/j.fbp.2012.08.006.
[69] J. Hategekimana, K.G. Masamba, J. Ma, F. Zhong, Encapsulation of vitamin E: effect of physicochemical properties of wall material on retention and stability, Carbohydr. Polym. 124 (2015) 172–179, https://doi.org/10.1016/j.carbpol.2015.01.060.
[70] M. Balakrishnan, S. Gayathiri, P. Preetha, R. Pandiselvam, G. Jeevarathinam, D.S.A. Delfiya, A. Kothakota, Microencapsulation of bixin pigment by spray drying: evaluation of characteristics, LWT–Food Sci. Technol. 145 (2021), 111343, https://doi.org/10.1016/j.lwt.2021.111343.
[71] A. Soottitantawat, K. Takayama, K. Okamura, D. Muranaka, H. Yoshii, T. Furuta, M. Ohkawara, P. Linko, Microencapsulation of l-menthol by spray drying and its release characteristics, Innovat. Food Sci. Emerg. Technol. 6 (2005) 163–170, https://doi.org/10.1016/J.IFSET.2004.11.007.
[72] N.L. Rozali, K.A. Azizan, R. Singh, S.N. Syed Jaafar, A. Othman, W. Weckwerth, U.S. Ramli, Fourier transform infrared (FTIR) spectroscopy approach combined with discriminant analysis and prediction model for crude palm oil authentication of different geographical and temporal origins, Food Control 146 (2023), https://doi.org/10.1016/j.foodcont.2022.109509.
[73] J. Yi, T.I. Lam, W. Yokoyama, L.W. Cheng, F. Zhong, Cellular uptake of beta-carotene from protein stabilized solid lipid nanoparticles prepared by homogenization-evaporation method, J. Agric. Food Chem. 62 (2014) 1096–1104, https://doi.org/10.1021/jf404073c.
[74] M.L.F.F. Ribeiro, Y.H. Roos, A.P.B. Ribeiro, V.R. Nicoletti, Effects of maltodextrin content in double-layer emulsion for production and storage of spray-dried carotenoid-rich microcapsules, Food Bioprod. Process. 124 (2020) 208–221, https://doi.org/10.1016/j.fbp.2020.09.004.
[75] T.A. Comunian, G. Grassmann Roschel, A.G. da Silva Anthero, I.A. de Castro, M. Dupas Hubinger, Influence of heated, unheated whey protein isolate and its combination with modified starch on improvement of encapsulated pomegranate seed oil oxidative stability, Food Chem. 326 (2020), 126995, https://doi.org/10.1016/j.foodchem.2020.126995.
[76] K.S. Yoha, J.A. Moses, C. Anandharamakrishnan, Refractance window drying: principles, applications, and emerging innovations, Drying Technology in Food Processing (2023) 417–455, https://doi.org/10.1016/B978-0-12-819895-7.00008-0.
[77] P.P. Shameena Beegum, M.R. Manikantan, K.B. Anju, V. Vinija, R. Pandiselvam, S. Jayashekhar, K.B. Hebbar, Foam mat drying technique in coconut milk: effect of additives on foaming and powder properties and its economic analysis, J. Food Process. Preserv. 46 (2022), e17122, https://doi.org/10.1111/JFPP.17122.